AGU PUBLICATIONS

Global Biogeochemical Cycles

RESEARCH ARTICLE
10.1002/2014GB004862

Key Points:
- The first high-resolution oceanic section of seawater dissolved Zn isotopes
- Sediments may be important sinks of isotopically light Zn from the oceans
- The deep ocean is homogeneous for Zn isotope ratios, except near sources

Supporting Information:
- Table S1

Correspondence to:
T. M. Conway,
conway.tm@gmail.com

Citation:
Conway, T. M., and S. G. John (2014), The biogeochemical cycling of zinc and zinc isotopes in the North Atlantic Ocean, *Global Biogeochem. Cycles, 28*, doi:10.1002/2014GB004862.

Received 26 MAR 2014
Accepted 19 SEP 2014
Accepted article online 23 SEP 2014

The biogeochemical cycling of zinc and zinc isotopes in the North Atlantic Ocean

Tim M. Conway[1,2] and Seth G. John[1]

[1]Department of Earth and Ocean Sciences, University of South Carolina, Columbia, South Carolina, USA, [2]Now at Institute for Geochemistry and Petrology, Department of Earth Sciences, ETH Zürich, Zürich, Switzerland

Abstract Zinc (Zn) is a marine micronutrient, with an overall oceanic distribution mirroring the major macronutrients, especially silicate. Seawater Zn isotope ratios (δ^{66}Zn) are a relatively new oceanographic parameter which may offer insights into the biogeochemical cycling of Zn. To date, the handful of published studies of seawater δ^{66}Zn show the global deep ocean to be both remarkably homogeneous (approximately +0.5‰) and isotopically heavier than the marine sources of Zn (+0.1 to +0.3‰). Here we present the first high-resolution oceanic section of δ^{66}Zn, from the U.S. GEOTRACES GA03 North Atlantic Transect, from Lisbon to Woods Hole. Throughout the surface ocean, biological uptake and release of isotopically light Zn, together with scavenging of heavier Zn, leads to large variability in δ^{66}Zn. In the ocean below 1000 m, δ^{66}Zn is generally homogeneous (+0.50 ± 0.14‰; 2 SD), though deviations from +0.5‰ allow us to identify specific sources of Zn. The Mediterranean Outflow is characterized by δ^{66}Zn of +0.1 to +0.3‰, while margin sediments are a source of isotopically light Zn (−0.5 to −0.8‰), which we attribute to release of nonregenerated biogenic Zn. Mid-Atlantic Ridge hydrothermal vents are also a source of light Zn (close to −0.5‰), though Zn is not transported far from the vents. Understanding the biogeochemical cycling of Zn in the modern ocean begins to address the imbalance between the light δ^{66}Zn signature of marine sources and the globally homogeneous deep oceans (δ^{66}Zn of +0.5‰) on long timescales, with overall patterns pointing to sediments as an important sink for isotopically light Zn throughout the oceans.

1. Introduction

Zinc (Zn) is a trace micronutrient in the oceans, utilized by phytoplankton in a range of enzymes, especially carbonic anhydrase and alkaline phosphatase [*Morel et al*., 1994; *Shaked et al*., 2006]. Dissolved Zn may therefore be an important control of distributions of surface productivity and the efficiency of the global carbon cycle. Globally, dissolved Zn has vertical oceanic profiles similar to macronutrients such as nitrate, phosphate, and silicate [*Bruland*, 1980], due to biological incorporation of Zn into phytoplankton in surface waters and regeneration of Zn deeper in the water column [e.g., *Lohan et al*., 2002]. In the deep ocean, average Zn concentrations increase from around 2–3 nmol kg^{-1} in the deep Atlantic to close to 10 nmol kg^{-1} in the deep Pacific [*Biller and Bruland*, 2012], as water masses age and accumulate nutrients from regenerating organic material. In the surface ocean, biological uptake often leads to low Zn concentrations, with as little as 15 pmol kg^{-1} within the surface mixed layer in Zn-depleted regions of the surface [*Wyatt et al*., 2014].

Since the first accurate measurements of dissolved Zn in the 1970s and 1980s [*Bruland et al*., 1978; *Bruland*, 1980], the similarity between the distribution of dissolved Zn and dissolved silicate has been remarked upon, with Zn and silicate both sharing deeper regeneration maxima than nitrate, phosphate, or other trace metals such as cadmium (Cd). This has led to hypotheses that Zn is present either within diatom silicate frustules or a more resistant organic refractory phase associated with the diatom frustule, either of which may regenerate more slowly throughout the water column, similar to opal [*Lohan et al*., 2002; *Zhao et al*., 2014]. However, studies suggest that only 1–3% of diatomaceous Zn is present within the silicate frustule, and most Zn is in fact located within the organic tissue of phytoplankton [*Ellwood and Hunter*, 2000; *Twining et al*., 2003, 2004], where it should be expected to regenerate in a similar way to the other algal nutrients. An alternative explanation for the similarity between Zn and silicate distribution in the ocean is that Zn may be scavenged onto the surface of sinking phytoplankton, causing it to be regenerated deeper than nitrate and phosphate, but at a depth more similar to silicate [*John and Conway*, 2014]. Finally, it has been proposed that the similar distribution of Zn and silicate is due to preferential biological uptake of Zn and silicate in high-productivity surface waters of the Southern Ocean, compared to nitrate and phosphate, resulting in a

relative deficit in Zn and silicate in Antarctic water masses that are advected northward to set the global distribution throughout the oceans [*Sarmiento et al*., 2004; *Wyatt et al*., 2014]. Accurate paired measurements of silicate and Zn concentrations are now becoming routine, especially as part of the GEOTRACES endeavor; however, many questions about the biogeochemical cycling of Zn, especially Zn's spatial incorporation into phytoplankton and the pathway via which Zn may be transported to and buried in sediments, remain unresolved.

Seawater-dissolved Zn stable isotope ratios (δ^{66}Zn) are a relatively new oceanographic parameter, which enable us to study the marine biogeochemical cycling and distribution of Zn. To date, the challenges of analysis have limited the measurement of dissolved seawater δ^{66}Zn to a handful of vertical profiles by just two laboratories. Despite the small number of profiles, measurements from the North Pacific, Atlantic, and Southern Oceans show the deep ocean to be remarkably homogeneous, with worldwide δ^{66}Zn of approximately +0.5‰ [*Bermin et al*., 2006; *Andersen et al*., 2011; *Boyle et al*., 2012; *Conway et al*., 2013; *Zhao et al*., 2014]. Intriguingly, a δ^{66}Zn value of +0.5‰ is heavier than both crustal Zn and the known inputs of Zn to the ocean (+0.1 to +0.3‰) [*Maréchal et al*., 2000; *Archer and Vance*, 2004; *Chapman et al*., 2006; *John et al*., 2007a; *Little et al*., 2014], indicative of a "missing" isotopically light sink of Zn from the oceans over timescales greater than the mixing time of the oceans [*Little et al*., 2014]. This light sink could take the form of burial of biogenic Zn [*Zhao et al*., 2014].

Within the surface ocean, variability in δ^{66}Zn has been previously attributed to several processes. The preferential acquisition of lighter Zn isotopes by phytoplankton has been observed both in culture and in lake settings, with experiments in culture showing intercellular Zn to be −0.2 to −0.8‰ lighter than the dissolved phase [*John et al*., 2007b; *Peel et al*., 2009; *John and Conway*, 2014], while adsorption of Zn to organic matter is likely to leave the dissolved phase isotopically lighter [*Gélabert et al*., 2006; *John and Conway*, 2014]. Increases in δ^{66}Zn toward the surface ocean have therefore typically been attributed to the preferential uptake of lighter Zn isotopes by phytoplankton, which leave the remaining dissolved phase isotopically heavy [*Bermin et al*., 2006; *Vance et al*., 2012; *John and Conway*, 2014; *Zhao et al*., 2014]. Measurements of δ^{66}Zn of core top diatom opal in the Southern Ocean showed a strong correlation with Zn/Si, inferred to represent increasing δ^{66}Zn as [Zn] concentrations decline [*Andersen et al*., 2011], although this pattern was not reproduced by more recent seawater δ^{66}Zn measurements in a surface transect from the Southern Ocean [*Zhao et al*., 2014]. A second major observation of Zn isotope studies is that a minimum in δ^{66}Zn has often been observed in subsurface waters [*Bermin et al*., 2006; *Vance et al*., 2012; *Zhao et al*., 2014], when it might be expected that the preferential incorporation of light isotopes into phytoplankton [*John et al*., 2007b] should lead to a monotonic increase in δ^{66}Zn, similar to that observed for δ^{114}Cd [*Ripperger et al*., 2007]. These excursions to low δ^{66}Zn values have been attributed either to regeneration of isotopically light intracellular Zn [*Vance et al*., 2012; *Zhao et al*., 2014] or due to scavenging of isotopically heavy Zn onto the surface of sinking organic particles [*John and Conway*, 2014]. In either case, Zn isotopes provide new information about the dynamic cycling of Zn in the surface ocean, as well as how biological uptake, scavenging, and regeneration influence the global distribution of zinc and its relationship with silicate and other macronutrients.

Here we present the first high-resolution paired oceanographic section of dissolved Zn concentration ([Zn]) and δ^{66}Zn across the North Atlantic Ocean. Five hundred and seventy six δ^{66}Zn measurements from 21 open ocean stations as part of the U.S. GEOTRACES GA03 North Atlantic Transect from Lisbon to Woods Hole, via Cape Verde, provide an order of magnitude increase in the δ^{66}Zn data available to investigate the marine biogeochemical cycling of Zn. Previously, a subset of surface data from this section was used by *John and Conway* [2014] as evidence for surface scavenging of heavy Zn. Here we use the full high-resolution GA03 section data set to refine our insights about the distribution of Zn and Zn isotopes in the oceans and scavenging and biological uptake/regeneration of Zn in the surface ocean. We identify new sources, sinks, and processes which lead to variability in [Zn] and δ^{66}Zn in the deep ocean, allowing us to constrain the relevance of margin sediments and hydrothermal vents to the global Zn budget and to gain a better understanding of the processes which control the global distribution of dissolved [Zn] and δ^{66}Zn.

2. Methods

2.1. Sampling

Atlantic seawater samples were collected as part of the U.S. GEOTRACES GA03 North Atlantic transect, on two cruises on board the R/V *Knorr* in October–November 2010 (USGT10) and November–December 2011 (USGT11). Twenty-one open ocean stations (25 to 37 point depth profiles) were sampled for dissolved [Zn]

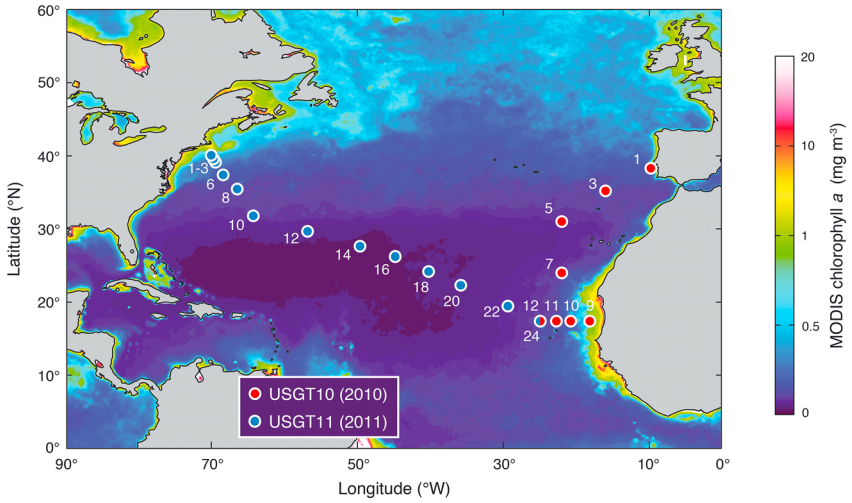

Figure 1. Station sampling locations in this study from the U.S. GEOTRACES GA03 North Atlantic transect. Both 2010 (USGT10) and 2011 (USGT11) cruise legs are shown. The station locations are shown overlain on the MODIS chlorophyll *a* (CHL_1) concentration (mg m^{-3}), averaged for the year 2011 (note nonlinear scale).

and δ^{66}Zn, eight in 2010 (USGT10-1, 3, 5, 7, 9, 10, 11, and 12) and thirteen in 2011 (USGT11-1, 2, 3, 6, 8, 10, 12, 14, 16, 18, 20, 22, and 24), with a crossover station at the Tenatso Time series close to Cape Verde (17.4°N, 2.45°W; USGT10-12, USGT11-24). Sampling locations are shown in Figure 1, overlain on the Moderate Resolution Imaging Spectroradiometer (MODIS) chlorophyll *a* concentration averaged for the year 2011. Samples were collected using published techniques [*Cutter and Bruland*, 2012] either into Go-Flow bottles on the GEOTRACES Rosette or by surface towfish (~2 m depth), and then filtered with 0.2 μm Pall Acropak-200 Supor cartridges into acid-cleaned 1 L polyethylene bottles. Samples were later acidified at the University of South Carolina to pH ~2 by addition of 1 mL 12 mol L^{-1} Aristar ultra hydrochloric acid and allowed to sit for at least 2 months before analysis of dissolved [Zn] and δ^{66}Zn.

2.2. Sample Processing and Analysis

Samples were processed and analyzed at the University of South Carolina according to published methods [*Conway et al.*, 2013]. All samples were processed in flow benches under ultralow particulate air filtration, all reagents were Aristar Ultra^{TM} obtained from VWR International, and all ultrapure water used was >18.2 MΩ. Dissolved [Zn] and δ^{66}Zn were measured at the Center for Elemental Mass Spectrometry at the University of South Carolina using a double-spike technique, following procedures detailed in *Conway et al.* [2013]. Briefly, seawater samples were spiked prior to processing with a ^{64}Zn–^{67}Zn double spike in an approximately 1:4 sample to spike ratio, and then Zn was quantitatively extracted onto Nobias PA-1 resin using a batch extraction technique in seawater adjusted to pH ~6.2. Zn was purified from Ni and major salts using AGMP-1 anion exchange resin, before analysis by a Thermo Neptune Multicollector-Inductively Coupled Plasma Mass Spectrometer (MC-ICPMS) in high-resolution mode, with a Pt Jet and Al "x type" skimmer cone. Samples were introduced via a borosilicate glass nebulizer and an ESI Apex-Q desolvation system without desolvating membrane. Each purified seawater sample was analyzed twice by MC-ICPMS, and an average value calculated for either [Zn] or δ^{66}Zn.

Dissolved [Zn] in each seawater sample was calculated by isotope dilution from addition of the double spike and the original weight of seawater, with 2% error assigned to account for pipetting and weighing error. Determination of [Zn] in SAFe S and D seawater standards, analyzed alongside North Atlantic samples, and reported elsewhere [*Conway et al.*, 2013], demonstrates excellent agreement with the most recent (May 2013) SAFe consensus values. Additionally, independent measurement of [Zn] in samples at five stations from the GA03 section by USC and UC Santa Cruz shows strong statistical agreement between laboratories, further demonstrating the excellent precision and accuracy of this technique (R. Middag, et al., GEOTRACES intercomparison of dissolved trace elements at the Bermuda Atlantic time series station, manuscript in preparation, 2014).

Dissolved δ^{66}Zn was calculated using a double-spike data reduction scheme based on the iterative approach of *Siebert et al.* [2001], as previously described [*Conway et al.*, 2013]. An in-house National Institute of Standards

and Technology (NIST) Standard Reference Material (SRM) 682 double-spike standard solution, with Zn concentration and sample:spike ratio both closely matching samples, was analyzed twice with each group of five to six samples, and then sample δ^{66}Zn was calculated relative to the mean of these two standards. Final sample δ^{66}Zn was then calculated by adjusting δ^{66}Zn values by −2.46‰ in order to express ratios relative to Lyon JMC Zn, based on repeated analysis of the separation between NIST SRM 682 and JMC, reported in *Conway et al*. [2013]. Thus, all stable Zn isotope ratios in this study are expressed relative to the Lyon JMC Zn isotope standard, in typical delta notation:

$$\delta^{66}\mathrm{Zn}\ (‰) = \left[\frac{\left(\frac{^{66}\mathrm{Zn}}{^{64}\mathrm{Zn}}\right)_{\mathrm{sample}}}{\left(\frac{^{66}\mathrm{Zn}}{^{64}\mathrm{Zn}}\right)_{\mathrm{JMC\,Lyon}}} - 1\right] \times 1000$$

Following *John* [2012] and *Conway et al*. [2013], the major source of uncertainty on stable isotope ratios obtained using the double-spike technique is internal analytical error, and so 2σ uncertainty on δ^{66}Zn measurements is expressed as the combined standard internal error of samples and bracketing standards, calculated as described previously [*Conway et al*., 2013]. Two sigma uncertainty is dependent on Zn concentration, with typical values of ~0.1‰ at 0.1 nmol kg^{-1} and ≤0.04‰ for seawater [Zn] at >0.5 nmol kg^{-1}. Our confidence in the accuracy of δ^{66}Zn measurements is reinforced by good agreement at the 2σ level of δ^{66}Zn of +0.5‰ in SAFe D1 and D2 samples, measured independently alongside the samples processed in this study and by the group at the University of Bristol and ETH Zürich using completely different chemical separation techniques and sample introduction desolvation systems on MC-ICPMS Neptune [*Conway et al*., 2013; *Zhao et al*., 2014].

2.3. Other Oceanographic Parameters

Macronutrients, dissolved oxygen, temperature, and salinity were measured on the GA03 section cruises using standard techniques and supplied by the Ocean Data Facility.

2.4. Data Processing and Calculations

Data for figures were processed using an in-house data interpolation scheme implemented in Matlab. For each station, values at all depths were first determined by 1-D linear interpolation from the data. Second, the vertically interpolated profiles were used as the basis of a 2-D linear interpolation to generate values across the entire GA03 section. For replicate analyses at the same depth, the mean value was used for figures. Samples from within a hydrothermal plume (>2400 m) that was sampled at the TAG hydrothermal site at Station USGT 11–16 at 44.83°W, 26.14°N on the Mid-Atlantic Ridge are not included in the plotted sections, because we regard these samples as reflecting plume waters which are unlikely to mix laterally with flanking stations, both due to bathymetry of the ridge valley and based on their temperature and salinity anomalies from the surrounding ocean.

Zn* is a parameter which can be used to highlight variability in the relationship between Zn and silicate (Si) in the ocean, which arises either as a result of sources or sinks with nonoceanic Zn/Si ratios, or biological uptake and regeneration of Zn and Si at different rates. We express Zn*, simplified from *Wyatt et al*. [2014] and analogous to Cd* [*Janssen et al*., 2014; *Conway and John*, 2014b] as

$$\mathrm{Zn}^{*} = [\mathrm{Zn}]_{\mathrm{measured}} - \left(\mathrm{Zn/Si}_{\mathrm{deep}} * [\mathrm{Si}]_{\mathrm{measured}}\right)$$

where $\mathrm{Zn/Si}_{\mathrm{deep}}$ is set at 0.06 to match the Zn/Si of deep waters in the east of the section (>3000 m; 25–40°W), which we regard as least influenced by local North Atlantic processes and closest to global deep ocean Zn/Si.

Isotope mass balance calculations in mixing calculations for two sources of Zn were performed using the following equation:

$$\delta^{66}\mathrm{Zn} = f_1 * \delta^{66}\mathrm{Zn}_1 + f_2 * \delta^{66}\mathrm{Zn}_2$$

where f_x and $\delta^{66}\mathrm{Zn}_x$ are the fraction and δ^{66}Zn contributed from each source.

3. Results

3.1. Oceanographic Setting, Dissolved Oxygen, and Macronutrients

The U.S. GEOTRACES GA03 North Atlantic transect, and the North Atlantic in general, with its proximity to potential sources of Zinc (sedimentary margins, aerosol dust, the Mediterranean Sea, and the Mid-Atlantic

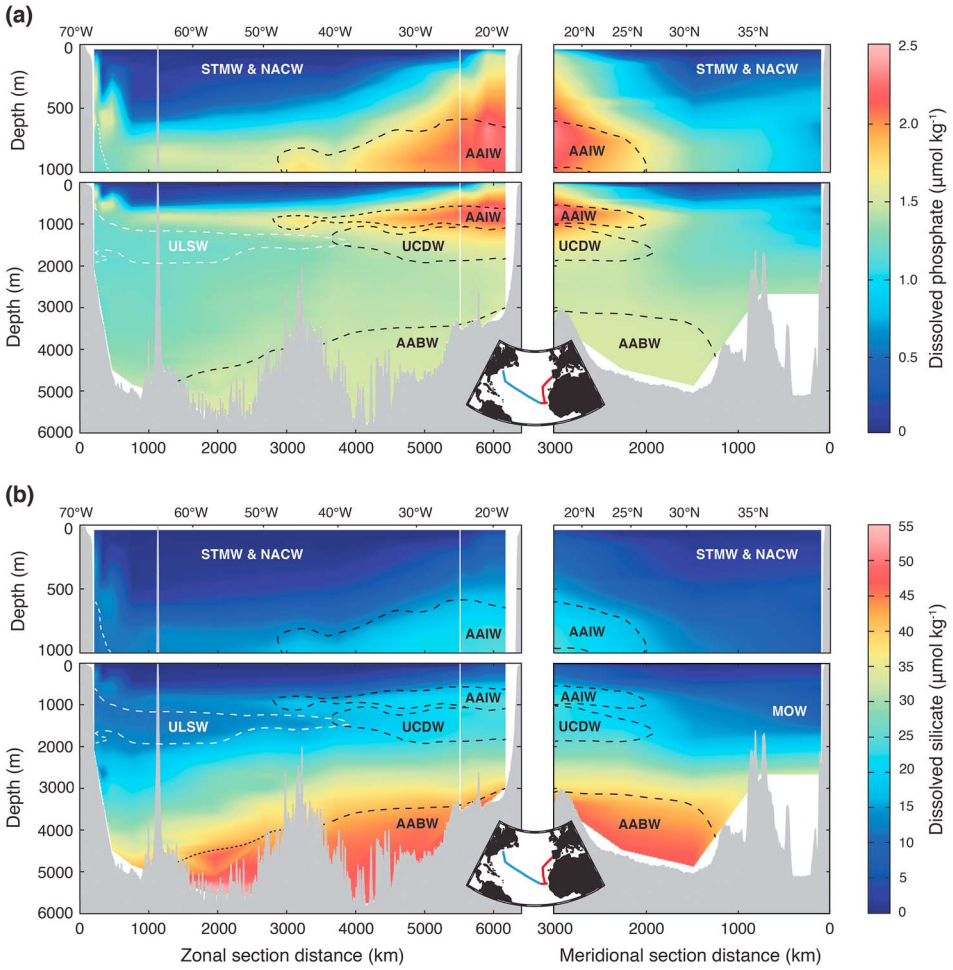

Figure 2. The Oceanographic Setting for the U.S. GEOTRCACES GA03 North Atlantic Transect. Dissolved (a) phosphate and (b) silicate concentrations are shown across the meridional and zonal sections. The crossover between 2010 and 2011 cruises is shown as a vertical white line. The influence of major Antarctic (black) and North Atlantic (white) water masses which influence the distribution of nutrients are shown. The position of Antarctic Intermediate Water (AAIW), Upper Circumpolar Deep Water (UCDW), Antarctic Bottom Water (AABW), and Upper Labrador Sea Water (ULSW) are indicated by the 40% (AAIW, UCDW), 50% (ULSW), or 30% (AABW) contribution contours calculated by *Jenkins et al.* [2014]. Nutrient-depleted surface water masses subtropical mode water (STMW), North Atlantic Central Water (NACW), and Mediterranean Outflow Water (MOW) are indicated by their white labels [*Jenkins et al.*, 2014; *Palter et al.*, 2005].

Ridge (MAR)), as well as the presence of a variety of both North Atlantic and southern-sourced water masses, provides an ideal section to study the cycling of Zn and δ^{66}Zn. The distribution of water masses described in this study is based on water mass analysis from the NAT cruise in *Jenkins et al.* [2014]. Dissolved phosphate and silicate distributions across the GA03 section are shown in Figure 2, along with their relationship to various water masses.

Dissolved phosphate and nitrate distributions across the GA03 section are most strongly influenced by the penetration of macronutrient-rich Antarctic Intermediate Water and Circumpolar Deep Water masses (AAIW, UCDW) through the basin at intermediate depths (~500–2000 m), most pronounced in the East (Figure 2a). In the west, from the North American margin to the Mid-Atlantic Ridge, nutrient-poor North Atlantic Deep Water masses, such as Upper Labrador Sea (ULSW), dominate the intermediate ocean, resulting in lower nitrate and phosphate concentrations in the deep western basin compared to eastern waters. In contrast to the other macronutrients, silicate concentrations are barely enriched within AAIW and UCDW, with the distribution of dissolved silicate influenced by surface biological uptake in the Antarctic that depletes silicate concentrations in these water masses [*Sarmiento et al.*, 2004]. Instead, silicate is most obviously related to the presence of Antarctic Bottom Water (AABW) in the deepest parts of the basin (>4000 m), where high silicate concentrations of $>40\,\mu mol\,kg^{-1}$ are found. Dissolved silicate is also depleted compared to nitrate and phosphate within the

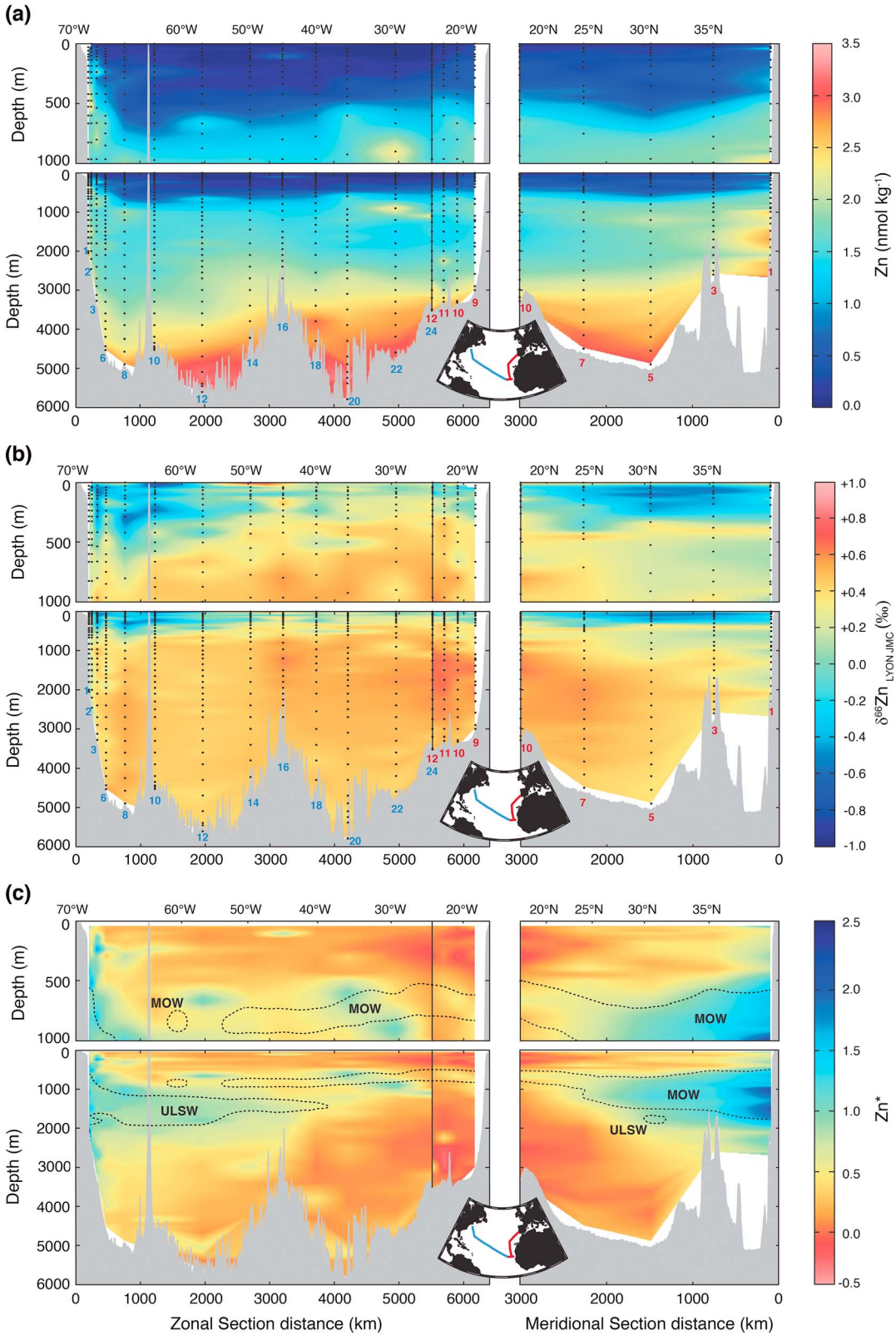

Figure 3. Dissolved Zn, δ^{66}Zn, and Zn* results from the U.S. GEOTRACES GA03 North Atlantic Transect. Station numbers are shown for USGT10 (red) and USGT11 (blue), with the cruise tracks for each leg shown in the small map panel. Crossover between the cruises at Stations USGT10-12/USGT11-24 is denoted by the black vertical lines. (a) Zn concentration, (b) δ^{66}Zn (‰) relative to Lyon JMC, and (c) Zn* (as calculated in the text). The influence of Upper Labrador Sea Water (ULSW) and Mediterranean Outflow Water (MOW) are shown by the dashed lines, based on the >50% contour for ULSW and the >30% contour for MOW as calculated by *Jenkins et al.* [2014].

water column close to Spain, where the Mediterranean Outflow supplies silicate-poor waters (Figure 2b). Across the entire basin, macronutrients are low in the upper ocean, where subtropical mode water (STMW) [*Palter et al.*, 2005], analogous to North Atlantic Central Water [*Jenkins et al.*, 2014], dominates above ~500 m in the west and shallows to the east. The surface water masses are depleted of macronutrients by biological uptake in situ in the surface ocean and within the STMW source regions [*Palter et al.*, 2005].

3.2. Distribution of Dissolved [Zn] and Zn*

Full GA03 sections for dissolved [Zn], δ^{66}Zn, and Zn* are shown in Figure 3, an expanded surface 1000 m shown in Figure 4, and samples from the hydrothermal plume at St. USGT11-16 shown in Figure 5. [Zn] are depleted throughout the surface ocean, with [Zn] of <1 nmol kg^{-1} above 500 m and reaching as low as 5–7 pmol kg^{-1} in towfish samples at the very surface. [Zn] generally increase with depth, with values increasing to up to 3.3 nmol kg^{-1} within the deepest waters (>5000 m). The increase in [Zn] with depth is consistent with both a "vertical" model of Zn distribution where Zn is depleted by biological uptake in the upper ocean and regenerated in the deep ocean and with a "horizontal" model where [Zn] are controlled by mixing from the Southern Ocean, such that high [Zn] are found in regions dominated by AABW, but not AAIW or UCDW, both of which are characterized by lower [Zn]. In contrast to other water masses in the upper ocean (<2000 m), where Zn is depleted relative to the macronutrients nitrate and phosphate, [Zn] are not depleted within ULSW. Higher [Zn] are also present within a few 100 km of both margins, and at depths ~500–2000 m throughout the meridional portion of the GA03 section where Mediterranean Outflow Water (MOW) dominates (Figures 3a and 3c), indicative of inputs of Zn in these regions. [Zn] up to 6.5 nmol kg^{-1} were measured within the hydrothermal plume at the TAG site on the Mid-Atlantic Ridge (Figure 5).

Zn* across the GA03 section ranges from -0.5 to +2 (Figure 3c), highlighting changes in the relationship between dissolved Zn and silicate concentrations. The most negative Zn* values are observed within and below the oxygen minimum zone close to North Africa extending to about 25°W and 20°N (100–500 m; Figures 3c, 4d, and 4e). Close to both margins, strongly positive Zn* are coincident with high [Zn], indicating a source of Zn but not silicate to the water column, most likely from sediments (Figures 3c, 6, and 7). ULSW and MOW water masses are also clearly picked out with high Zn*, suggesting that these young North Atlantic water masses are enriched in Zn relative to silicate, and therefore overall sources of Zn to the oceanic inventory. MOW, especially, is characterized by high [Zn] and low silicate, suggesting a significant contribution of Zn to the North Atlantic from the outflow, which we observe from close to Spain to as far south as 19°N. The lack of any significant Zn* near the MAR, outside of the hydrothermal plume, suggests that the ridge vents do not have a significant impact on the oceanic dissolved Zn budget in the North Atlantic.

3.3. Distribution of Zn Isotopes

Seawater dissolved zinc stable isotope ratios (δ^{66}Zn) across the GA03 section range from -1.1‰ to +0.9‰ (Figures 3–8), representing a larger range than previously published (~0.9‰; [*Zhao et al.*, 2014]) for seawater. The surface 100 m shows the most variability in δ^{66}Zn (-1.1‰ to +0.9‰; Figure 4c), although we acknowledge that extremely low Zn concentrations (<0.1 nmol kg^{-1}) and higher 2σ uncertainty (>0.1‰) most likely contribute to this range. However, deeper in the surface ocean (100–1000 m), where [Zn] are higher and uncertainty is lower, we still observe variability in δ^{66}Zn from -0.6‰ to +0.6‰ (Figures 3b and 4c). For the whole GA03 section below 1000 m, the ocean is relatively homogeneous for δ^{66}Zn (mean δ^{66}Zn of $+0.45 \pm 0.24$‰; 2 SD $n = 267$). Even within the deep ocean, however, there is variability in δ^{66}Zn within this section, from -0.2‰ to +0.7‰. Lighter δ^{66}Zn values (<0.3‰) are observed nearer both margins (Figures 3b, 4c, 6, and 7), within the hydrothermal plume (Figure 5), and within MOW (Figure 6). Heavier δ^{66}Zn values (>0.5‰) are observed closer to West Africa (Figures 3b and 8). After excluding stations close to both margins (USGT10-1, 3; USGT11-1 to -6) and the hydrothermal plume samples (USGT11-16) the deep ocean is remarkably homogeneous for δ^{66}Zn (mean $+0.50 \pm 0.14$‰; 2 SD, $n = 202$), indistinguishable from deep ocean δ^{66}Zn values of ~+0.5‰ reported previously from the Pacific, Atlantic, Indian, and Southern Oceans [*Bermin et al.*, 2006; *Andersen et al.*, 2011; *Conway et al.*, 2013; *Zhao et al.*, 2014].

4. Discussion

A wide variety of different biogeochemical processes contribute to the observed δ^{66}Zn throughout the GA03 section. These processes include those that cycle Zn and δ^{66}Zn within the ocean, such as

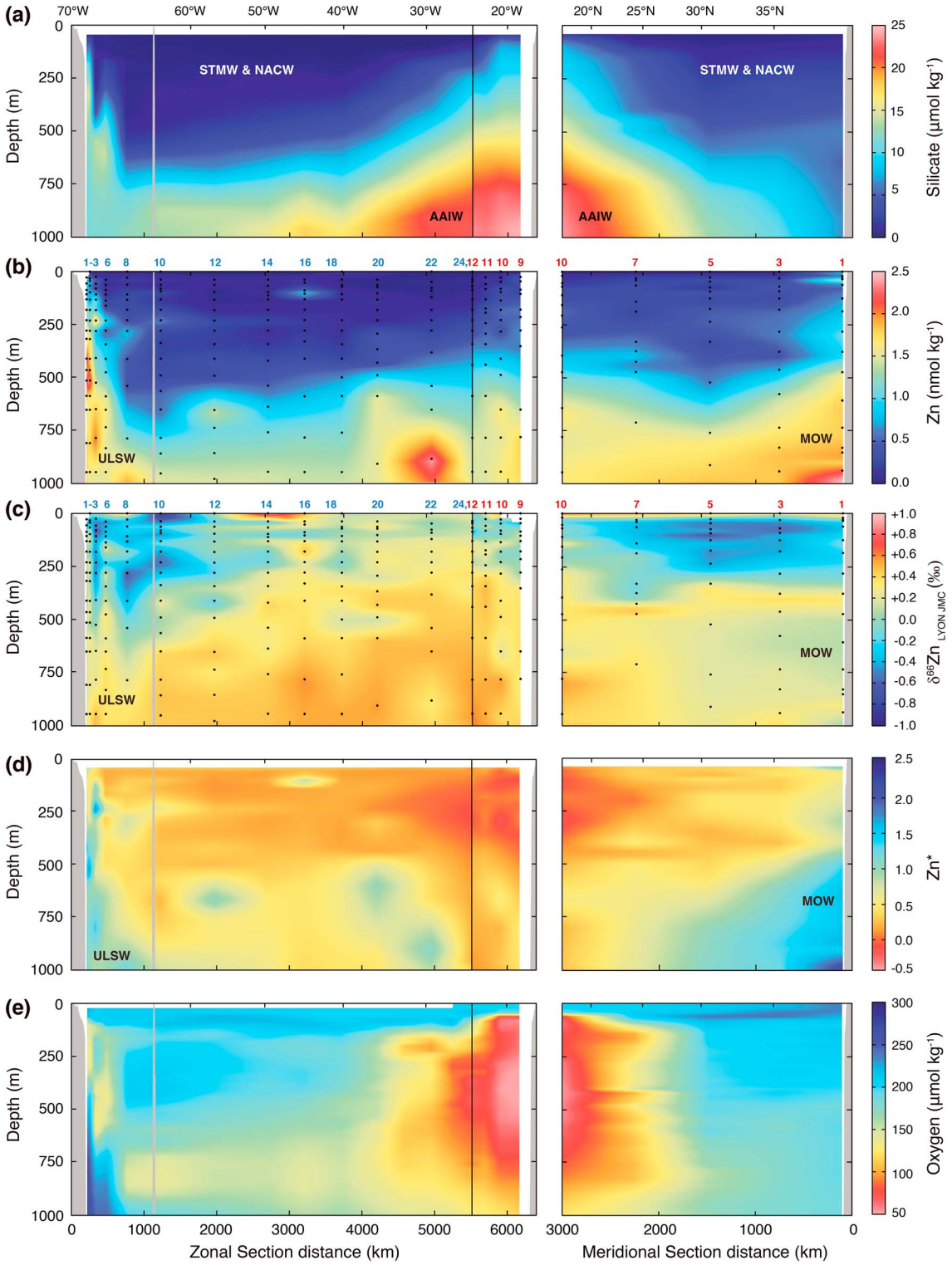

Figure 4. Data for multiple dissolved parameters throughout the top 1000 m of the U.S. GEOTRACES GA03 North Atlantic Transection (a) silicate concentration, (b) Zn concentration, (c) δ^{66}Zn (‰) relative to Lyon JMC, (d) Zn* (as calculated in the text), and (e) oxygen concentration. Station numbers are shown for USGT10 (red) and USGT11 (blue). Crossover between the cruises at Stations USGT10-12/USGT11-24 is denoted by the black vertical lines. Influences of major water masses are labeled: Subtropical mode water and North Altantic Central Water (STMW and NACW), Antarctic Intermediate Water (AAIW), Upper Labrador Sea Water (ULSW), and Mediterranean Outflow Water (MOW) [*Jenkins et al.*, 2014; *Palter et al.*, 2005].

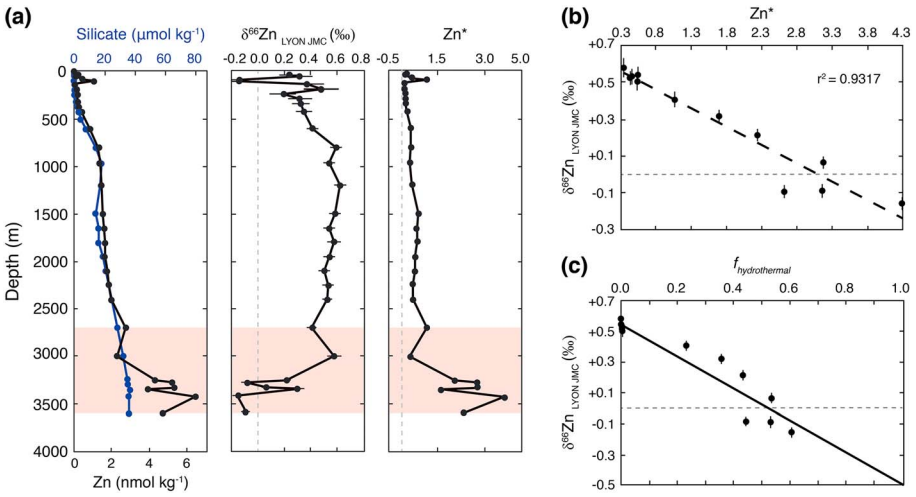

Figure 5. The influence of the TAG hydrothermal vents for dissolved Zn. (a) Dissolved Zn and silicate concentration, δ^{66}Zn (‰) relative to Lyon JMC, and Zn* (as calculated in the text) are shown for USGT11-16 above the TAG hydrothermal site on the Mid-Atlantic Ridge at 26.1°N, 44.8°W. (b) The δ^{66}Zn (‰) plotted against Zn* for samples at USGT11-16 below 1900 m, with a dashed line of best fit. (c) The δ^{66}Zn (‰) plotted against the calculated fraction ($f_{hydrothermal}$) of the dissolved Zn in each sample that was contributed by the hydrothermal vents (as calculated in the text). Simple two-component mixing between an oceanographic Zn end-member (δ^{66}Zn of +0.54‰) and a hypothetical hydrothermal Zn end-member (δ^{66}Zn of −0.5‰), as calculated in the text, is represented by the solid black line. Error bars are 2σ, as described in section 2. The red-shaded area represents the depth at which the hydrothermal plume influences dissolved Zn.

biological uptake and regeneration, and those that constitute sources and sinks for the marine Zn cycle, adding or removing Zn from the ocean. In the following discussion we consider these processes and then go on to discuss specific regions of the GA03 section where these processes are most clearly observed. These regions include (1) the oligotrophic surface ocean, (2) the OMZ close to West Africa, (3) the meridional (north-south) eastern portion of the GA03 section near the Mediterranean outflow, (4) the American margin including the continental shelf and western basin, (5) the region of hydrothermal venting on the Mid-Atlantic ridge, and (6) the entire deep basin focusing on differences in δ^{66}Zn from west to east.

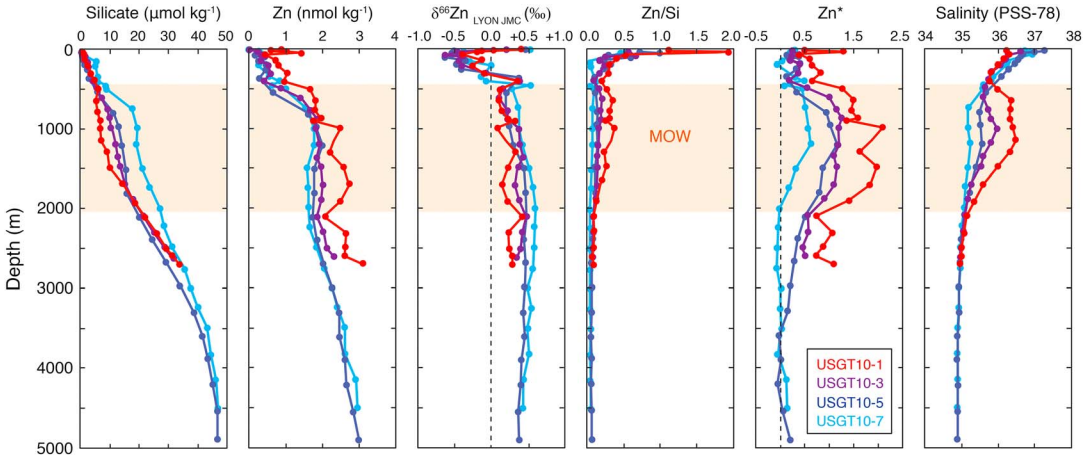

Figure 6. Depth profiles for multiple dissolved parameters from GA03 meridional stations USGT10-1 to USGT10-7. Silicate and zinc concentrations, δ^{66}Zn (‰) relative to Lyon JMC, Zn/Si ratio (nmol μmol^{-1}), Zn* (as calculated in the text), and salinity are shown. For clarity, error bars are not shown, but 2σ error below 200 m is <0.05‰ (see supporting information). The depth interval at which Mediterranean OutflowWaters (MOW) influences the stations, based on salinity, is shown by the shaded orange horizon.

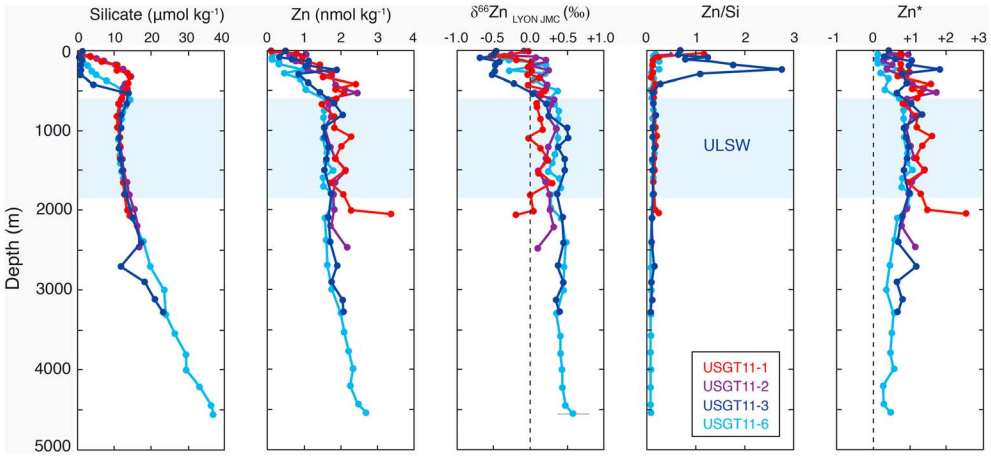

Figure 7. Depth profiles for multiple dissolved parameters from GA03 North American margin stations USGT11-1 to USGT11-6. Silicate and zinc concentrations, δ^{66}Zn (‰) relative to Lyon JMC, Zn/Si ratio (nmol μmol^{-1}), and Zn* (as calculated in the text). For clarity, error bars are not shown for most depths, but 2σ error is typically $<$0.07‰ (see supporting information). The depth interval at which Upper Labrador Seawater (ULSW) influences the stations is shown by the shaded blue horizon, based on Figure 2.

4.1. Processes That May Affect δ^{66}Zn

Patterns of dissolved [Zn] and δ^{66}Zn throughout the surface ocean likely reflect the fractionation of the dissolved Zn reservoir due to the influence of four distinct surface processes:

1. Uptake of Zn into phytoplankton cells, which has been shown both in culture and in vivo to preferentially incorporate light Zn isotopes [*John et al*., 2007b; *Peel et al*., 2009; *John and Conway*, 2014], leaving the residual dissolved Zn isotopically heavier.
2. Release of biogenic Zn with depth as organic matter regenerates, releasing light Zn and acting to bring the seawater δ^{66}Zn back to the "original" value, assuming complete dissolution. Rapid regeneration of intracellular light Zn, either from cell lysis and degradation within the water column [*John and Conway*, 2014], or potentially in discrete examples as a consequence of cells bursting during filtration, could be responsible for regions of discrete light δ^{66}Zn throughout the surface, as suggested for other oceanic regions [*Vance et al*., 2012; *Zhao et al*., 2014].
3. Scavenging of Zn to organic particle surfaces, with studies showing that heavy Zn isotopes are preferentially scavenged [*Gélabert et al*., 2006; *John and Conway*, 2014]. Scavenging would leave the residual dissolved Zn pool isotopically lighter [*John and Conway*, 2014]. Although scavenged Zn may only constitute a small fraction of the total Zn ($<$1%) at any one time, simple one-dimensional modeling demonstrates that scavenging may have a large effect on δ^{66}Zn and could be the cause of excursions to isotopically light dissolved seawater δ^{66}Zn observed in the subsurface [*John and Conway*, 2014].
4. Finally, it is possible that Zn is removed from the dissolved phase as Zn sulfides precipitate associated with microenvironments around sinking biological particles in low-oxygen regions. This was recently proposed for both Cd and Zn in oxygen deficient zones of the open ocean, where dissolved oxygen is low ($<$100 μmol kg^{-1}), but waters are not anoxic [*Janssen et al*., 2014]. ZnS precipitation might be expected to preferentially remove light Zn isotopes into the particulate phase, by analogy with CdS, leaving the dissolved phase isotopically heavy.

Dissolved [Zn] or Zn* may give some guide to which of these processes is dominating the δ^{66}Zn of the dissolved Zn pool in different regions of the surface ocean, with increases in [Zn] and Zn* pointing to the regeneration of biomass and release of light intercellular Zn [*Vance et al*., 2012; *Zhao et al*., 2014], while scavenging and/or ZnS precipitation expected to remove Zn relative to silicate, leading to low [Zn] and low Zn*. In comparison to the simple δ^{66}Zn profiles reported for other oceans [*Bermin et al*., 2006; *Vance et al*., 2012; *Zhao et al*., 2014], the more complicated δ^{66}Zn picture in the North Atlantic suggests that the balance between these processes may vary dependent on oceanographic conditions.

In the intermediate and deep ocean δ^{66}Zn is likely to be dominated by the regeneration or removal to sediments of scavenged heavy Zn, assimilated light Zn, and hypothesized ZnS phases, as well as addition

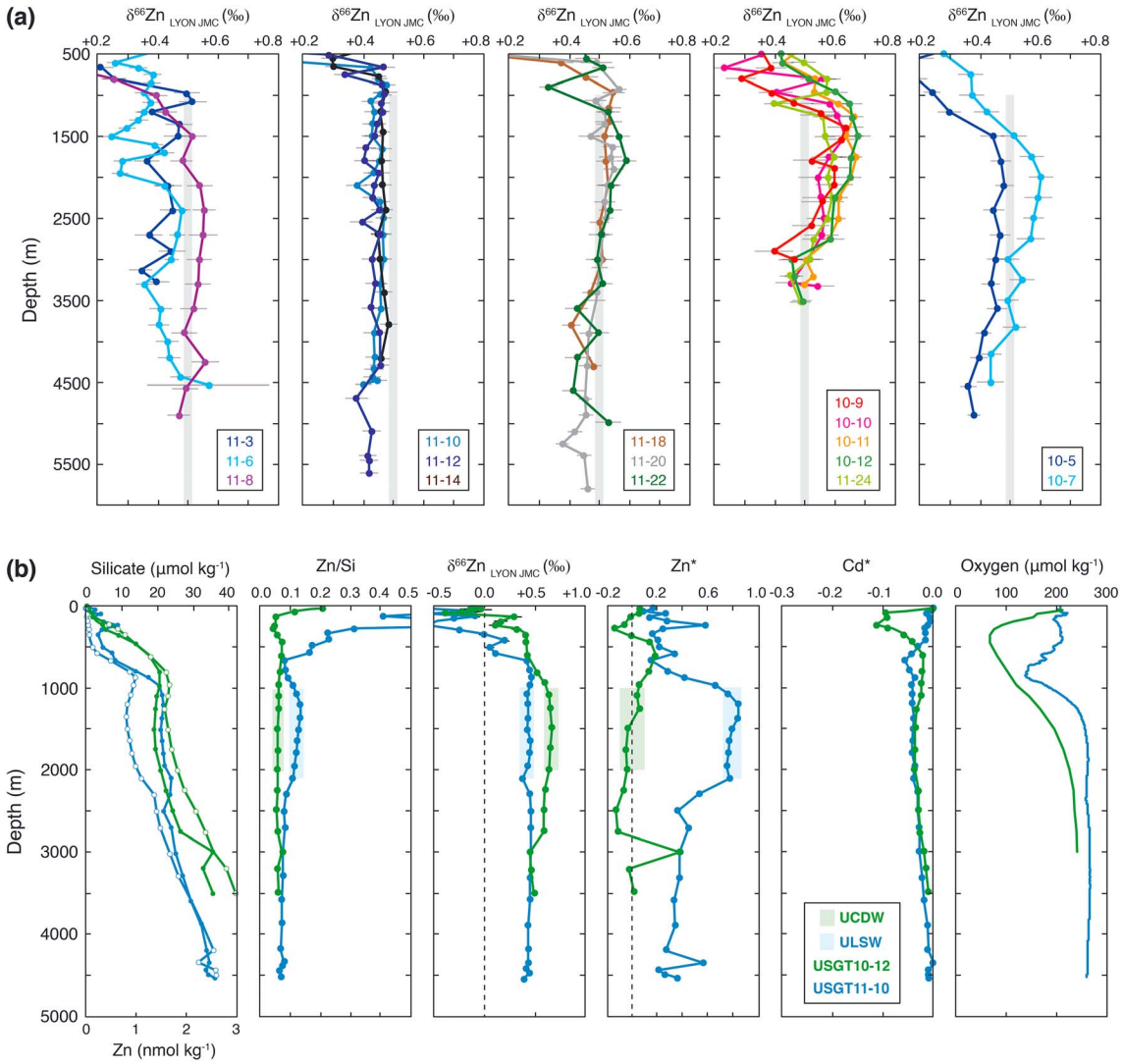

Figure 8. Variability in multiple dissolved parameters from west to east across the U.S. GEOTRACES GA03 North Atlantic Transect. (a) Dissolved δ^{66}Zn depth profiles for multiple stations across the section, showing variability in δ^{66}Zn in the deep ocean. The shaded grey boxes indicate 2 SD around the deep ocean mean for δ^{66}Zn below 1000 m (0.50 ± 0.14‰), as calculated from open ocean data in this study (excluding margin stations USGT10 1–3 and USGT11 1–6). (b) Comparison of typical western and eastern North Atlantic depth profiles for several dissolved parameters. Station USGT11-10 (31.8°N, 64.2°W), close to Bermuda, is shown in blue, and station USGT10-12 (17.4°N, 24.5°W), close to West Africa, is shown in green. Silicate (open circles) and zinc (closed circles) concentrations, dissolved Zn/Si ratio (nmol μmol^{-1}), δ^{66}Zn (‰) relative to Lyon JMC, Zn* (as calculated in the text), Cd* (*Conway and John* [2014b] as defined by *Janssen et al.* [2014]), and oxygen concentration are shown. The depths of the influence of Upper Labrador Seawater in the west and Upper Circumpolar Deep Water in the east, based on Figure 2, are shown as blue- and green-shaded boxes, respectively. Two sigma error bars are shown for δ^{66}Zn, as described in section 2; error bars for other parameters are smaller than the size of the points.

ofZn from discrete sources. From the GA03 section, we have identified three important local sources of Zn to the deep Atlantic that appear to significantly affect dissolved δ^{66}Zn. The first is Mediterranean outflow water, the second is margin sediments, and the third is hydrothermal venting. Below, we discuss how these sources, combined with the four biological processes discussed above, set dissolved ocean δ^{66}Zn in six different regions of the North Atlantic.

4.2. Regional Biogeochemical Cycling of Zn and δ^{66}Zn in the North Atlantic

4.2.1. The Oligotrophic Upper Ocean

The predominant water mass in the upper ~500 m of the North Atlantic is subtropical mode water (STMW; Figures 2 and 4a). STMW is a warm and saline water mass formed in the North Atlantic driven by evaporation over the warmer months and deep mixing in the winter [*Palter et al.*, 2005]. As a consequence of high productivity in the source regions of this water mass, STMW is depleted in all of the macronutrients as well as Zn.

Previously, using a subset of the data presented here, a pattern of low δ^{66}Zn in the upper ~500 m of the North Atlantic was identified [*John and Conway*, 2014], with occasional increases in δ^{66}Zn in the surface 2 m of the ocean. The expanded data set presented here matches these previous observations, with lower δ^{66}Zn observed within the upper ~500 m at all 21 stations measured (−0.6 to +0.2‰), compared to values at 1000 m (~+0.5‰). A significant excursion to higher δ^{66}Zn in the surfacemost sample (2 m), which was observed at just one station in the previous data set, is observed in nine stations in this expanded data set of the full GA03 section. In fact, the pattern is seen most clearly throughout the meridional portion of the GA03 section (Figures 4c and 6), where the surface 500 m of all four meridional stations (USGT10-1, 3, 5, and 7) are characterized by a pattern of heavier δ^{66}Zn at the very surface (+0.2 to +0.5‰), a broad excursion to light δ^{66}Zn values of −0.4 to −0.6‰ around 50–200 m, and a return to +0.5‰ at 350–500 m, before declining into the region where MOW strongly influences Zn (discussed in section 4.2.4). This pattern in δ^{66}Zn in these four stations is accompanied by a gradual increase in [Zn], and with the exception of the margin station USGT10-1, similar Zn* values throughout this depth interval at these stations are consistent with gradual release of Zn from phytoplankton rather than discrete pulses of intracellular light Zn. Therefore, consistent with the interpretation of our previous study [*John and Conway*, 2014], we suggest that the overall observed pattern in δ^{66}Zn throughout the surface 500 m is the result of biological uptake at the surface driving δ^{66}Zn to heavier values, with scavenging of Zn to organic matter creating regions of isotopically light δ^{66}Zn within the subsurface, and δ^{66}Zn values returning to oceanic (+0.5‰) with depth when sufficient cellular and adsorbed Zn have regenerated.

In some surface samples in this expanded data set (18 samples from <500 m at USGT11-3, 6, 8 and 10), light δ^{66}Zn (+0.1 to −0.7‰) is clearly associated with high Zn* (+0.3 to +1.8 cf. < +0.3 for most of the top 500 m across the zonal section; Figures 4c and 4d), suggesting regeneration of intracellular light Zn close to the surface, as previously proposed [*Vance et al*., 2012; *Zhao et al*., 2014], or a source of sedimentary Zn close to the margins, which is discussed in later sections. This feature is observed most clearly closest to the North American margin, where the four closest stations (USGT11-1, 2, 3, and 6), which also fall along Line W [*Toole et al*., 2011], display intriguing features within the top 500 m (Figure 7). There is a dramatic shift to high Zn*, low silicate, and light δ^{66}Zn between USGT11-2 (39.4°N, 69.5°W) and 3 (38.7°N, 69.1°W), most prominently observed at ~250 m (Figure 7), which is likely to reflect crossing the boundary of the Gulf Stream which intersects line W close to these stations [*Toole et al*., 2011]. The influence of the warm gulf stream may be responsible for the pronounced region of low macronutrients, high [Zn] and light δ^{66}Zn through the top 300 m at USGT11-3 (Figure 7), while stations USGT1-1 and 2 are more strongly influenced by the margin and upwelling of deeper water brings oceanic Zn and nutrients closer to the surface at USGT11-8 (Figure 4a). The presence of higher concentrations of isotopically light Zn within the Gulf Stream, compared to relative depletion of other nutrients may point to the transport of regenerated light intracellular Zn from high-productivity regions farther south.

The fact that the patterns in δ^{66}Zn over the upper 1000 m for all 21 stations in this study match the patterns observed for the five stations studied previously suggests that the processes which govern Zn biogeochemical cycling in STMW, and perhaps the North Atlantic as a whole, have a major influence on δ^{66}Zn throughout the upper North Atlantic. Other features observed in the upper 1000 m of the water column, including the input of isotopically light Zn from sediments near both margins and in Mediterranean outflow water, will be discussed below.

4.2.2. The Eastern Basin Oxygen Minimum Zone

Close to West Africa, where surface productivity is high, a pronounced oxygen minimum zone (OMZ) is present in the subsurface ocean, extending from roughly 100 m to 1000 m, and extending westward to approximately 35°W (Station USGT11-20) and as far as 27°N (Figure 4e). The OMZ is characterized by low O_2 (<120 μmol kg^{-1}) and high macronutrient (nitrate and silicate) concentrations, which reflect both the presence of the nutrient-rich AAIW water mass and the high productivity in surface waters of this region with subsequent regeneration of sinking organic matter. Zn concentrations are relatively low, compared to silicate, both within the OMZ and below the OMZ, resulting in the lowest Zn* values of the entire transect, which is likely to be due, in part, to the preferential removal of Zn in the Southern Ocean source regions for AAIW, compared to other nutrients [*Wyatt et al*., 2014]. Additionally, low Zn* may point to a preferential removal process for Zn compared to silicate within the surface North Atlantic.

In this region of high biogenic particle flux, a variety of different particle interactions may affect dissolved δ^{66}Zn. First, as in other surface waters across the GA03 section, we observe a decrease in δ^{66}Zn in the upper

~500 m, with occasional increases in δ^{66}Zn at the very surface, consistent with both biological uptake and scavenging of Zn to particles. Second, it is possible that Zn sulfides are precipitated in microenvironments around sinking biogenic particles within low-oxygen waters, particularly at the top of the OMZ, as has been recently proposed for Cd [*Janssen et al*., 2014], based on anomalously low Cd* and high-particulate Cd concentrations in this region. Similarly, ZnS precipitation should lead to a decrease in Zn*, because Zn is removed by a process which does not affect silicate, and an increase in δ^{66}Zn, because sulfide precipitation is expected to preferentially remove light Zn isotopes [*Archer et al*., 2004]. Indeed, we do observe the lowest values of Zn* anywhere in the GA03 section associated with the top of the OMZ and a minimum in Cd* (Figure 8b), as well as the highest values of δ^{66}Zn in the eastern basin associated with low Zn* in waters below the OMZ. An increase to heavier δ^{66}Zn is not observed associated with the OMZ itself, but this could be due to other processes influencing δ^{66}Zn at these depths. Zn and δ^{66}Zn are also affected by scavenging onto sinking particles, which is likely to be more intense in this region of high biological activity, and is likely to have the opposite effect on dissolved δ^{66}Zn to ZnS formation. It is possible that scavenging of heavy Zn is obscuring the isotopic effect of ZnS precipitation on δ^{66}Zn within the core of the OMZ. Alternatively, it could be that ZnS are not formed in these low oxygen waters and the observed Zn* and δ^{66}Zn have other causes; the lighter δ^{66}Zn values within the OMZ are perhaps most consistent with intense Zn scavenging, and the higher δ^{66}Zn values below the OMZ could be caused by the release of isotopically heavy scavenged Zn.

4.2.3. Margin Sedimentary Zn Sources

In stations close to both the North American and Iberian margins, we observe excursions to higher [Zn], and δ^{66}Zn values lighter than the oceanographic background (approximately +0.5‰), which provide the first clear evidence that sediments are a significant local source of isotopically light Zn to the deep Atlantic Ocean.

At station USGT10-1, the station closest to Spain, we see a clear input of Zn from the Iberian margin (Figure 6). High [Zn] and Zn* are observed all the way through the water column, especially directly above the sediments, coincident with the lightest δ^{66}Zn in the deep meridional portion of the GA03 section (+0.07 to +0.09‰). This sedimentary input does not appear to change smoothly with depth over the profile, and it has no clear relationship to transmissometry (indicative of particle load). Instead, we observe several discrete maxima in [Zn] and Zn*, each of which is associated with a minimum in δ^{66}Zn (Figure 6). By comparing δ^{66}Zn between 1000 m and 1700 m from the most northern and most southern stations along the meridional transect (USGT10-1 and USGT10-7, respectively) a simple isotope mass balance calculation can be used to infer the δ^{66}Zn signature of the locally sourced sedimentary Zn. Assuming that both the differences in δ^{66}Zn between USGT10-1 and USGT10-7 at ~1000 m (+0.07 ± 0.03‰ versus +0.37 ± 0.04‰) and ~1700 m (+0.13 ± 0.03‰ versus +0.57 ± 0.03‰) and the excess Zn (0.74 and 1.09 nmol kg^{-1} at station USGT10-1 at ~1000 m and ~1700 m) are the result of local sedimentary Zn addition to the water column, the sedimentary Zn sources have calculated δ^{66}Zn signatures of −0.53 ± 0.10 and −0.65 ± 0.15‰, respectively.

Similar sedimentary Zn inputs are observed at the stations closest to the North American margin, where high [Zn] and Zn* are coincident with low δ^{66}Zn. Again, these inputs are not smoothly distributed over the profile; instead, they appear as maxima in Zn* which appear at a single sampling depth or several depths, each of which is associated with a minimum in δ^{66}Zn. On the North American margin, the most dramatic change in Zn* and δ^{66}Zn is observed just above the sediments at USGT11-1, where a dramatic increase in [Zn] to 3.38 nmol kg^{-1} is accompanied by a δ^{66}Zn of −0.19‰, compared to [Zn] and δ^{66}Zn values of 2.28 nmol kg^{-1} and +0.04‰ for the sample taken just 50 m higher in the water column. This excursion in both [Zn] and δ^{66}Zn close to the sediments, as well as lighter δ^{66}Zn values (close to 0‰) at multiple depths at station USGT11-1, suggests the presence of an isotopically light sedimentary source on the North American margin, similar to that seen close to Spain. Indeed, a similar isotope mass balance calculation to that made on the Iberian margin, based instead on data from ~2100 m at USGT11-1 and USGT11-6 (3.38 ± 0.07 versus 1.57 ± 0.03 nmol kg^{-1} and −0.19 ± 0.03 versus +0.42 ± 0.03‰) suggests that the sedimentary source of Zn on the North American margin is characterized by a δ^{66}Zn of −0.72 ± 0.07‰, similar to the signature inferred in the east (−0.53 to −0.65‰).

One possible explanation for this isotopically light sedimentary source is that light Zn may be released from degrading phytoplankton material within the sediments. Along the Iberian margin, the inferred offset between surface ocean δ^{66}Zn (+0.4‰ and +0.03 at 2 and 23 m, respectively) and sedimentary δ^{66}Zn (−0.5 to −0.7‰) is −0.5 to −1.1‰, similar to the reported fractionation by two different species of cultured marine phytoplankton

under high-Zn conditions, which would be typical of coastal upwelling regimes [*John et al*., 2007b; *John and Conway*, 2014]. Similarly, on the North American margin, surface δ^{66}Zn values at USGT11-1 are −0.04‰ at 2 m and −0.22‰ at 30 m, and the inferred sedimentary Zn source is −0.72‰, an offset of −0.5 to −0.7‰. These calculated values are also consistent with a best fit δ^{66}Zn value of −0.3‰, or possibly as light as −0.85‰, for sinking particulate organic matter, inferred from demosponge spicules in the Southern Ocean [*Hendry and Andersen*, 2013]. Thus, one possible explanation for the release of isotopically light Zn from sediments is that a significant portion of the Zn that is assimilated by phytoplankton growing near continental margins, where productivity is high and Zn is not completely depleted in surface waters by biological productivity (allowing large biological fractionations to be expressed), could be transferred to the sediments. This is in contrast to the oligotrophic ocean, where Zn supplied to the euphotic zone is nearly quantitatively removed into phytoplankton, and we expect the assimilated δ^{66}Zn to match dissolved δ^{66}Zn at the base of the euphotic zone, without an opportunity for large biological fractionations to be expressed.

Alternatively, the release of isotopically light Zn from the sediments might be due to the release of Zn trapped in sinking particles as isotopically light Zn sulfides (section 4.2.2). For example, it could be that Zn precipitates as ZnS within the anoxic microenvironments surrounding biogenic particles in the water column but is later released within the sediments as those particles become further degraded and the environment around them becomes completely oxic.

It is not yet clear which processes on both margins lead to a transfer of isotopically light Zn to the sediments. Equally, it is not yet clear what causes isotopically light Zn to be released to the water column, either through release of pore water dissolved Zn or resuspension of sedimentary colloids, the latter of which has been suggested to be an important source of dissolved Fe in this region [*Fitzsimmons et al*., 2014]. However, regardless of the processes, it is likely that there are other sedimentary environments in which this same light Zn pool is present but not released to the water column. In environments where pore waters are reducing or sulfidic, this light Zn may instead be retained within sediments and not returned to the ocean. Thus, a local source of isotopically light Zn from sediments in the North Atlantic may point toward processes that are ultimately a sink of light Zn from the global ocean on long timescales.

4.2.4. Mediterranean Outflow

In addition to the evidence of biological Zn cycling in the surface (section 4.2.1) and sedimentary inputs (section 4.2.3), Zn isotope ratios along the meridional (north-south) portion of the GA03 section suggest input of Zn from Mediterranean Outflow Water (MOW). In Figures 3 and 6, the influence of MOW can be clearly seen at depths of ~500–2000 m as a region of higher [Zn] and high Zn* (+1 to +2.5), characterizing MOW as a high Zn, low silicate water mass (Figure 6), with δ^{66}Zn values of +0.1 to +0.3‰. These δ^{66}Zn values are lighter than the deep ocean (approximately +0.5‰), but similar to riverine, continental, and anthropogenic Zn (+0.1 to +0.4‰; [*Maréchal et al*., 2000; *John et al*., 2007a; *Little et al*., 2014]). We therefore regard the young salty Mediterranean waters as being dominated by nonoceanographic Zn from some combination of rivers, sediments, and anthropogenic sources. The δ^{66}Zn signature of MOW is also consistent with measurements of δ^{66}Zn from acid mine drainage feeding the Rio Tinto and Rio Odiel Rivers (+0.1 to +0.4‰) and possibly the Gulf of Cadiz via the Huelva Estuary [*Borrok et al*., 2008]. This anthropogenic Zn source has been proposed to be a significant contribution to high [Zn] in surface waters close to Spain and also the Western Mediterranean and therefore potentially also MOW [*van Geen et al*., 1997, and references therein; *Nieto et al*., 2007; *Borrok et al*., 2008].

Figures 3 and 6 clearly show the waning influence of MOW southward along the meridional transect as MOW mixes with the background ocean, with salinity, [Zn] and Zn* all falling, and δ^{66}Zn increasing along the GA03 section from stations USGT10-1 to USGT10-7. In the zonal portion of the GA03 section, the influence of MOW is still discernible in both the high [Zn] and low δ^{66}Zn in a number of places in the ~500–2000 m depth range across nearly the entire basin as far as 60°W (Figure 3).

4.2.5. Mid-Atlantic Ridge

At the TAG site on the Mid-Atlantic Ridge (44.8°W, 26.1°N), as is the case for dissolved Fe [*Conway and John*, 2014a], hydrothermal venting appears to be a source of dissolved Zn to the water column, with [Zn] of 3–7 nmol kg^{-1} which is clearly enriched above the background "oceanographic" Zn (~2 nmol kg^{-1}) within the region of the hydrothermal plume at station USGT11-16 (Figure 5a). Clear enrichment of [Zn] and Zn*, (Figure 5), are coincident with excursions to lighter δ^{66}Zn, indicative of an isotopically light hydrothermal

contribution to the dissolved phase. A strong negative correlation between [Zn] and δ^{66}Zn (Figure 5b) throughout 1950–3600 m suggests that dissolved Zn within the plume can be largely explained by mixing between oceanic Zn (~2 nmol kg^{-1}) and a hydrothermal component. Fitting a simple two-component modeling (Figure 5c) line to the data, using a nonhydrothermal Zn contribution, linearly extrapolated downward from samples above the plume's influence, with a δ^{66}Zn of +0.54‰, suggests that the hydrothermal end-member is most closely approximated by a δ^{66}Zn value of −0.5‰.

Both the lightest δ^{66}Zn value within the plume (−0.16 ± 0.04‰; 2σ) and the hypothesized −0.5‰ hydrothermal Zn end-member are notably lighter than both white (+0.13 to +0.31‰) and black (0.0 to +0.25‰) smoker fluids measured directly from TAG [*John et al*., 2008], as well as source basalts (+0.2 to +0.3‰; [*John et al*., 2008, and references therein]). Previously, large variations (−0.4 to +1.3‰) in δ^{66}Zn have been reported from hydrothermal deposits [*Mason et al*., 2005; *Wilkinson et al*., 2005], with precipitation of ZnS within hydrothermal systems thought to strongly influence the δ^{66}Zn of the black/white smoker fluids [*John et al*., 2008]. It therefore seems likely that the lighter δ^{66}Zn signal in the plume is the result of fractionation of the dissolved phase due to nonquantitative ZnS precipitation from the original hydrothermal fluids, which are known to have μmol kg^{-1} dissolved Zn; however, ZnS formation should drive $\delta^{66}Zn_{dissolved}$ to heavier values, with isotope effects of $\Delta\delta^{66}$Zn estimated to range from −0.36‰ under laboratory conditions and from 0 to −0.87‰ in hydrothermal samples from the East Pacific Rise [*Archer et al*., 2004; *John et al*., 2008]. This suggests that the hydrothermal Zn contribution may not be truly dissolved but could instead comprise largely of nanoparticulate Zn sulfides that were precipitated from the vent fluids, traveled within the plume, but are included within the operationally defined "dissolved" (<0.2 μm) phase.

Deviation from the simple two-component modeling line in Figure 5c could point toward variability in the hydrothermal end-member, perhaps indicative of three-component mixing between oceanic Zn (+0.5‰), a nanoparticulate ZnS phase (−0.5‰), and a dissolved contributed from the original vent fluids (0 to +0.2‰). Alternatively, some scavenging or precipitation of dissolved hydrothermal or oceanic Zn within the plume, as is seen for Cd in these samples [*Conway and John*, 2014b], could cause deviations in δ^{66}Zn from a simple mixing line. Although it is clear that more work is required to understand the chemistry of Zn within hydrothermal settings, we show here, for the first time, that Zn released into the water column from North Atlantic hydrothermal vents is significantly lighter than would be predicted from hydrothermal fluids. Data from above TAG at USGT11-16 and from the nearby west and east stations at USGT11-14 (27.6°N, 49.6°W) and USGT11-18 (24.2°N, 40.2°W) suggest that this hydrothermal δ^{66}Zn signal does not persist far from the vent itself and may not even spread outside the plume (Figure 3).

4.2.6. Variability Within the Open Deep Ocean

Away from the influence of margin sediments, the deep Atlantic Ocean is relatively homogeneous in δ^{66}Zn, around a deep ocean mean of +0.5‰ (Figure 3b). Despite this overall homogeneity, however, small amplitude but systematic variability in δ^{66}Zn is observed moving across the zonal portion of the GA03 section from west to east (Figure 8a, left to right), and through the meridional portion of the GA03 section from north to south (Figure 8a, right-hand panel). Stations in the western half of the basin (USGT11-10, USGT11-12, and USGT11-14) have strikingly homogeneous vertical profiles for δ^{66}Zn, close to +0.45‰, while those in the east have pronounced "bulges" in δ^{66}Zn to values of up to +0.6 to +0.7‰ between 1000 and 2500 m (Figure 8a). In fact, the zonal portion is characterized by a gradual transition from straight profiles with δ^{66}Zn less than the deep ocean mean (represented by the grey bar in Figure 8a) in the west, through profiles close to the mean in the central basin, to those with heavier δ^{66}Zn excursions at intermediate depths in the east. A similar transition is seen from USGT10-5 and 10-7 southward in the Meridional Transect (Figure 8a, right). This intriguing pattern suggests variability in the local sources and sinks of dissolved Zn across the GA03 section. There are several possibilities that could explain the overall change in δ^{66}Zn across the GA03 section, and direct comparison of [Zn], Zn*, Zn/Si, and δ^{66}Zn between representative western and eastern profiles is informative (Figure 8b). Most simply, the transition in δ^{66}Zn from west to east can be interpreted by either addition of heavy Zn or removal of light Zn in the east creating a "bulge" in δ^{66}Zn in the east, or the addition of light Zn or removal of heavy Zn at the same depths in the west masking a "bulge" in δ^{66}Zn in the west.

Addition of a large source of heavy Zn in the east, perhaps carried by UCDW which dominates this depth horizon (Figures 2 and 8b), is inconsistent with Zn*, which is much lower in the east than in the west (Figure 8b). Additionally, all known potential sources of Zn to the water column are ≤+0.5‰, with sediments

close to crustal or isotopically light, aerosols and rivers at +0.3 to +0.4‰ [*Little et al*., 2014], and hydrothermal Zn isotopically light. Finally, the UCDW end-member, sampled in the Southern Ocean has a δ^{66}Zn signature of close to +0.5‰ [*Zhao et al*., 2014]. Thus, instead of interpreting the higher δ^{66}Zn in the eastern basin as the addition of heavy Zn, we might interpret it as resulting from water column loss of isotopically light Zn, for example, by sulfide precipitation associated with the oxygen minimum zone near the African margin or due to incomplete regeneration of assimilated Zn in organic matter, both of which could be removed to sediments, leaving the water column isotopically heavy.

Alternatively, the dramatic increase in Zn* and relatively lower δ^{66}Zn in the western basin near the North American margin may be due to input of isotopically light Zn throughout ULSW, near the North American margin (Figure 8b). Viewed in this context, the addition of isotopically light Zn from USLW in the west may be partially overprinting an excursion to higher δ^{66}Zn such as is observed in eastern profiles. If this is the case, a "bulge" toward heavier values in the subsurface might in fact represent a more typical oceanographic profile for δ^{66}Zn, away from the influence of young north Atlantic water masses that are carrying a crustal or sedimentary Zn component. In fact, a similar small-amplitude "bulge" in δ^{66}Zn can be observed in two published profiles from the Southern Ocean, associated with lower Circumpolar Deep Water [*Zhao et al*. 2014, Figures 7 and 8], as well as at similar depths in a single profile from the North Pacific (T. M. Conway, unpublished data, 2014), suggesting that this profile shape could be widespread for oceanic δ^{66}Zn. If this shape is typical of oceanic Zn profiles, it may actually be attributable to regeneration of scavenged heavy Zn at intermediate depths within the oceans, which is being masked in the Western North Atlantic by the slight sedimentary input of dissolved Zn.

4.3. Implications for the Global Oceanic Mass Balance of Zn and Zn Isotopes

Based on this work, there are several implications for understanding the global oceanic mass balance of Zn, especially the homogeneity of the deep ocean, when the known inputs of Zn, continental, riverine, and aerosol δ^{66}Zn are close to +0.3‰ and the known outputs, in the form of carbonates, ferromanganese nodules, and ferromanganese crusts are isotopically heavy (+0.9 to +1‰; [*Maréchal et al*., 2000; *Pichat et al*., 2003; *Little et al*., 2014]).

1. Our data suggest that hydrothermal venting is unlikely to represent a large source of Zn to the oceans and does not account for the +0.5‰ signature of the deep ocean. We have characterized MAR vents as a source of isotopically light Zn (−0.5‰) to the oceans, and we show that this Zn does not disperse far from the vents.
2. We have found direct evidence of a light sedimentary Zn reservoir (inferred δ^{66}Zn of −0.5 to −0.8‰). While we observe that some of this reservoir is released back into the water column, acting as a local source of Zn, incomplete release or burial of this isotopically light sedimentary Zn in other environments could constitute a light sink of Zn from the oceans. It is possible that this sedimentary reservoir comprises of assimilated biological Zn which is not fully regenerated within the water column, constituting a light biogenic sink for Zn from the oceans [*Little et al*., 2014; *Zhao et al*., 2014]. Alternatively, based on Zn* and Cd* under low-oxygen conditions in this region, we have hypothesized that ZnS precipitation could be occurring within low-oxygen waters in the Atlantic, constituting another possible water column sink for isotopically light Zn. A balance of external inputs of Zn to the oceans with these two hypothesized sedimentary sinks for light Zn, over timescales longer than the mixing of the oceans, may explain the globally homogeneous heavy ocean at +0.5‰.
3. If ZnS precipitation does occur associated with OMZs, the magnitude of this flux would be expected to be highly sensitive to the global distribution and extent of OMZs, which would be expected to change over time with patterns of global productivity, ocean circulation, and global climate. Thus, if ZnS precipitation does constitute a significant sink for dissolved Zn, it would imply that the ocean δ^{66}Zn might not be in steady state over geological timescales. Future studies focusing on OMZs in the Pacific and Indian Oceans will no doubt provide more insight into whether ZnS precipitation is important for the global marine Zn budget.

5. Conclusions

We have presented the first high-resolution oceanographic section of dissolved [Zn] and δ^{66}Zn in the oceans, from the U.S. GEOTRACES GA03 Transect through the North Atlantic Ocean. This section provides a wealth of

data on the distribution of Zn and δ^{66}Zn in the North Atlantic, which we have used to provide new insights into the oceanographic and biogeochemical controls on the marine cycling of Zn and Zn isotopes in this region. Our data also support earlier work suggesting the overall homogeneity of the global deep oceans for δ^{66}Zn at close to +0.5‰ but also show that there is significant variability in δ^{66}Zn associated with specific biogeochemical processes and regions of the North Atlantic. Data from this work support the findings of our previous study, which suggests that a balance between biological assimilation of Zn and scavenging of Zn to particles explain the overall pattern of δ^{66}Zn variations in surface waters. For the first time, we have characterized and identified local sources of Zn to the North Atlantic, with the Mediterranean Outflow characterized by near-crustal δ^{66}Zn, sedimentary sources on both margins with an inferred δ^{66}Zn of −0.5 to −0.8‰ and hydrothermal Zn from MAR vents with a δ^{66}Zn of −0.5‰. Lastly, we have suggested that an isotopically light sediment Zn reservoir provides evidence of a burial flux of isotopically light Zn, supporting ideas that this could be a light sink balancing external inputs of Zn to the ocean over long timescales resulting in a homogeneous deep ocean for δ^{66}Zn.

Acknowledgments

Dissolved [Zn] and δ^{66}Zn data presented in this study are deposited with the Biological and Chemical Oceanography Data Management Office and are also available as supporting information. We thank the Captain, crew and GEOTRACES sampling team on board the R/V *Knorr* on both USGT10 and USGT11 cruises. We also thank Angela Rosenberg and Beth Bair for technical assistance with analysis, Ken Bruland, Rob Middag, and Jingfeng Wu for supplying concentration data that informed double-spike calculations. We thank two anonymous reviewers for their comments and insight that helped us to improve this manuscript. The Ocean Data Facility supplied macronutrients and oceanographic parameters from the cruises. Figures were generated using Matlab and Adobe Illustrator. This study was funded by NSF grant OCE-1131387. A subset of this data set was previously published by *John and Conway* [2014].

References

Andersen, M. B., D. Vance, C. Archer, R. F. Anderson, M. J. Ellwood, and C. S. Allen (2011), The Zn abundance and isotopic composition of diatom frustules, a proxy for Zn availability in ocean surface seawater, *Earth Planet. Sci. Lett.*, *301*(1–2), 137–145, doi:10.1016/j.epsl.2010.10.032.

Archer, C., and D. Vance (2004), Mass discrimination correction in multiple-collector plasma source mass spectrometry: An example using Cu and Zn isotopes, *J. Anal. Atom. Spectrom.*, *19*, 656–665, doi:10.1039/B315853E.

Archer, C., D. Vance, and I. Butler (2004), Abiotic Zn isotope fractionations associated with ZnS precipitation, *Geochim. Cosmochim. Acta*, *68*(11), A325–A325, doi:10.1016/j.gca.2004.05.008.

Bermin, J., D. Vance, C. Archer, and P. J. Statham (2006), The determination of the isotopic composition of Cu and Zn in seawater, *Chem. Geol.*, *226*(3–4), 280–297, doi:10.1016/j.chemgeo.2005.09.025.

Biller, D. V., and K. W. Bruland (2012), Analysis of Mn, Fe, Co, Ni, Cu, Zn, Cd, and Pb in seawater using the Nobias-chelate PA1 resin and magnetic sector inductively coupled plasma mass spectrometry (ICP-MS), *Mar. Chem.*, *130–131*, 12–20, doi:10.1016/j.marchem.2011.12.001.

Borrok, D. M., D. A. Nimick, R. B. Wanty, and W. I. Ridley (2008), Isotopic variations of dissolved copper and zinc in stream waters affected by historical mining, *Geochim. Cosmochim. Acta*, *72*(2), 329–344, doi:10.1016/j.gca.2007.11.014.

Boyle, E. A., S. John, W. Abouchami, J. F. Adkins, Y. Echegoyen-Sanz, M. Ellwood, A. R. Flegal, K. Fornace, C. Gallon, and S. Galer (2012), GEOTRACES IC1 (BATS) contamination-prone trace element isotopes Cd, Fe, Pb, Zn, Cu, and Mo intercalibration, *Limnol. Oceanogr. Meth.*, *10*, 653–665, doi:10.4319/lom.2012.10.653.

Bruland, K. W. (1980), Oceanographic distributions of cadmium, zinc, nickel, and copper in the North Pacific, *Earth Planet. Sci. Lett.*, *47*(2), 176–198, doi:10.1016/0012-821X(80)90035-7.

Bruland, K. W., G. A. Knauer, and J. H. Martin (1978), Zinc in Northeast Pacific water, *Nature*, *271*(5647), 741–743, doi:10.1038/271741a0.

Chapman, J. B., T. F. D. Mason, D. J. Weiss, B. J. Coles, and J. J. Wilkinson (2006), Chemical separation and isotopic variations of Cu and Zn from five geological reference materials, *Geostand. Geoanal. Res.*, *30*(1), 5–16, doi:10.1111/j.1751-908X.2006.tb00907.x.

Conway, T. M., and S. G. John (2014a), Quantification of sources of dissolved iron to the North Atlantic Ocean, *Nature*, *511*, 212–215, doi:10.1038/nature13482.

Conway, T. M., and S. G. John (2014b), Biogeochemical cycling of cadmium isotopes along a high-resolution section through the North Atlantic Ocean, *Geochim. Cosmochim. Acta*, doi:10.1016/j.gca.2014.09.032.

Conway, T. M., A. D. Rosenberg, J. F. Adkins, and S. G. John (2013), A new method for precise determination of iron, zinc and cadmium stable isotope ratios in seawater by double-spike mass spectrometry, *Anal. Chim. Acta*, *793*, 44–52, doi:10.1016/j.aca.2013.07.025.

Cutter, G. A., and K. W. Bruland (2012), Rapid and noncontaminating sampling system for trace elements in global ocean surveys, *Oceanogr. Limnol. Meth.*, *10*, 425–436, doi:10.4319/lom.2012.10.425.

Ellwood, M. J., and K. A. Hunter (2000), The incorporation of zinc and iron into the frustule of the marine diatom Thalassiosira pseudonana, *Limnol. Oceanogr.*, *45*(7), 1517–1524, doi:10.4319/lo.2000.45.7.1517.

Fitzsimmons, J. N., G. G. Carrasco, J. Wu, M. Roshan, M. Hatta, C. I. Measures, T. M. Conway, S. G. John, and E. A. Boyle (2014), Partitioning of dissolved iron and iron isotopes into soluble and colloidal phases along the U.S. GEOTRACES North Atlantic Transect, *Deep Sea Res., Part II*, in press.

Gélabert, A., O. S. Pokrovsky, J. Viers, J. Schott, A. Boudou, and A. Feurtet-Mazel (2006), Interaction between zinc and freshwater and marine diatom species: Surface complexation and Zn isotope fractionation, *Geochim. Cosmochim. Acta*, *70*(4), 839–857, doi:10.1016/j.gca.2005.10.026.

Hendry, K. R., and M. B. Andersen (2013), The zinc isotopic composition of siliceous marine sponges: Investigating nature's sediment traps, *Chem. Geol.*, *354*, 33–41, doi:10.1016/j.chemgeo.2013.06.025.

Janssen, D. J., T. M. Conway, S. G. John, J. Christian, D. I. Kramer, T. F. Pederson, and J. T. Cullen (2014), Undocumented water column sink for cadmium in open ocean oxygen deficient zones, *Proc. Natl. Acad. Sci.*, *111*(19), 6888–6893, doi:10.1073/pnas.1402388111.

Jenkins, W. I., W. M. Smethie, E. A. Boyle, and G. C. Cutter. (2014), Water mass analysis for the U.S. GEOTRACES North Atlantic sections, *Deep Sea Res., Part II*, in press.

John, S. G. (2012), Optimizing sample and spike concentrations for isotopic analysis by double-spike ICPMS, *Anal. Atom. Spectrom.*, *27*, 2123–2131, doi:10.1039/c2ja30215b.

John, S. G., and T. M. Conway (2014), A role for scavenging in the marine biogeochemical cycling of zinc and zinc isotopes, *Earth Planet. Sci. Lett.*, *394*, 159–167, doi:10.1016/j.epsl.2014.02.053.

John, S. G., J. Genevievepark, Z. Zhang, and E. A. Boyle (2007a), The isotopic composition of some common forms of anthropogenic zinc, *Chem. Geol.*, *245*(1–2), 61–69, doi:10.1016/j.chemgeo.2007.07.024.

John, S. G., R. W. Geis, M. A. Saito, and E. A. Boyle (2007b), Zinc isotope fractionation during high-affinity and low-affinity zinc transport by the marine diatom Thalassiosira oceanica, *Limnol. Oceanogr.*, *52*(6), 2710–2714, doi:10.4319/lo.2007.52.6.2710.

John, S. G., O. J. Rouxel, P. R. Craddock, A. E. Engwall, and E. A. Boyle (2008), Zinc stable isotopes in seafloor hydrothermal vent fluids and chimneys, *Earth Planet. Sci. Lett.*, *269*(1–2), 17–28, doi:10.1016/j.epsl.2007.12.011.

Little, S. H., D. Vance, C. Walker-Brown, and W. M. Landing (2014), The oceanic mass balance of copper and zinc isotopes, investigated by analysis of their inputs, and outputs to ferromanganese oxide sediments, *Geochim. Cosmochim. Acta*, *125*, 673–693, doi:10.1016/j.gca.2013.07.046.

Lohan, M. C., P. J. Statham, and D. W. Crawford (2002), Total dissolved zinc in the upper water column of the subarctic North East Pacific, *Deep Sea Res., Partt II*, *49*(24–25), 5793–5808, doi:10.1016/S0967-0645(02)00215-1.

Maréchal, C. N., E. Nicolas, C. Douchet, and F. Albarède (2000), Abundance of zinc isotopes as a marine biogeochemical tracer, *Geochem. Geophys. Geosyst.*, *1*, 1015, doi:10.1029/1999GC000029.

Mason, T. F. D., D. J. Weiss, J. B. Chapman, J. J. Wilkinson, S. G. Tessalina, B. Spiro, M. S. A. Horstwood, J. Spratt, and B. J. Coles (2005), Zn and Cu isotopic variability in the Alexandrinka volcanic-hosted massive sulphide (VHMS) ore deposit, Urals, Russia, *Chem. Geol.*, *221*(3–4), 170–187, doi:10.1016/j.chemgeo.2005.04.011.

Morel, F. M. M., J. R. Reinfelder, S. B. Roberts, C. P. Chamberlain, J. G. Lee, and D. Yee (1994), Zinc and carbon co-limitation of marine phytoplankton, *Nature, 369*(6483), 740–742, doi:10.1038/369740a0.

Nieto, J. M., A. M. Sarmiento, M. Olias, C. R. Canovas, I. Riba, J. Kalman, and T. A. Delvalls (2007), Acid mine drainage pollution in the Tinto and Odiel Rivers (Iberian Pyrite Belt, SW Spain) and bioavailability of the transported metals to the Huelva estuary, *Environ. Int.*, *33*(4), 445–455, doi:10.1016/j.envint.2006.11.010.

Palter, J. B., M. S. Lozier, and R. T. Barber (2005), The effect of advection on the nutrient reservoir in the North Atlantic subtropical gyre, *Nature*, *437*(7059), 687–692, doi:10.1038/nature03969.

Peel, K., D. Weiss, and L. Sigg (2009), Zinc isotope composition of settling particles as a proxy for biogeochemical processes in lakes: Insights from the eutrophic Lake Greifen, Switzerland, *Limnol. Oceanogr.*, *54*(5), 1699–1708, doi:10.4319/lo.2009.54.5.1699.

Pichat, S., C. Douchet, and F. Albarède (2003), Zinc isotope variations in deep-sea carbonates from the eastern equatorial Pacific over the last 175 ka, *Earth Planet. Sci. Lett.*, *210*(1–2), 167–178, doi:10.1016/S0012-821X(03)00106-7.

Ripperger, S., M. Rehkämper, D. Porcelli, and A. N. Halliday (2007), Cadmium isotope fractionation in seawater - A signature of biological activity, *Earth Planet. Sci. Lett.*, *261*(3–4), 670–684, doi:10.1016/j.epsl.2007.07.034.

Sarmiento, J. L., N. Gruber, M. A. Brzezinski, and J. P. Dunne (2004), High-latitude controls of thermocline nutrients and low latitude biological productivity, *Nature*, *427*(6969), 56–60, doi:10.1038/nature02127.

Shaked, Y., Y. Xu, K. Leblanc, and F. M. M. Morel (2006), Zinc availability and alkaline phosphatase activity in Emiliania huxleyi: Implications for Zn-P co-limitation in the ocean, *Limnol. Oceanogr.*, *51*(1), 299–309, doi:10.4319/lo.2006.51.1.0299.

Siebert, C., T. F. Nagler, and J. D. Kramers (2001), Determination of molybdenum isotope fractionation by double-spike multicollector inductively coupled plasma mass spectrometry, *Geochem. Geophys. Geosyst.*, *2*, 1032, doi:10.1029/2000GC000124.

Toole, J. M., R. G. Curry, T. M. Joyce, M. McCartney, and B. Peña-Molino (2011), Transport of the North Atlantic Deep Western Boundary Current about 39°N, 70°W: 2004–2008, *Deep Sea Res., Part II*, *58*(17–18), 1768–1780, doi:10.1016/j.dsr2.2010.10.058.

Twining, B. S., S. B. Baines, N. S. Fisher, J. Maser, S. Vogt, C. Jacobsen, A. Tovar-Sanchez, and S. A. Sanudo-Wilhelmy (2003), Quantifying trace elements in individual aquatic protist cells with a synchrotron X-ray fluorescence microprobe, *Anal. Chem.*, *75*(15), 3806–3816, doi:10.1021/ac034227z.

Twining, B. S., S. B. Baines, and N. S. Fisher (2004), Element stoichiometries of individual plankton cells collected during the Southern Ocean Iron Experiment (SOFeX), *Limnol. Oceanogr.*, *49*(6), 2115–2128, doi:10.4319/lo.2004.49.6.2115.

Vance, D., Y. Zhao, J. Cullen, and M. Lohan (2012), Zinc isotopic data from the NE Pacific reveals shallow recycling, *Mineral. Mag.*, *76*(6), 2486.

van Geen, A., J. F. Adkins, E. A. Boyle, C. H. Nelson, and A. Palanques (1997), A 120-yr record of widespread contamination from mining of the Iberian pyrite belt, *Geology*, *25*(4), 291–294, doi:10.1130/0091-7613(1997)025<0291:AYROWC>2.3.CO;2.

Wilkinson, J. J., D. J. Weiss, T. F. D. Mason, and B. J. Coles (2005), Zinc isotope variation in hydrothermal systems: Preliminary evidence from the Irish Midlands ore field, *Econ. Geol.*, *100*(3), 583–590, doi:10.2113/gsecongeo.100.3.583.

Wyatt, N. J., A. Milne, E. M. S. Woodward, A. P. Rees, T. J. Browning, H. A. Bouman, P. J. Worsfeld, and M. C. Lohan (2014), Biogeochemical cycling of dissolved zinc along the GEOTRACES South Atlantic transect GA10 at 40°S, *Global Biogeochem. Cy.*, *28*(1), 44–56, doi:10.1002/2013GB004637.

Zhao, Y., D. Vance, W. Abouchami, and H. J. W. de Baar (2014), Biogeochemical cycling of zinc and its isotopes in the Southern Ocean, *Geochim. Cosmochim. Acta*, *125*, 653–672, doi:10.1016/j.gca.2013.07.045.